THERMAL DESIGN OF INFLATABLE SPHERICAL SHADOW SHIELDS

by D. G. McConnell and J. P. Campbell

Lewis Research Center
Cleveland, Ohio

NATIONAL AERONAUTICS AND SPACE ADMINISTRATION

THERMAL DESIGN OF INFLATABLE SPHERICAL SHADOW SHIELDS

by D. G. McConnell and J. P. Campbell

Lewis Research Center
National Aeronautics and Space Administration
Cleveland, Ohio

ABSTRACT

This paper presents the heat transfer from a spherical balloon type shadow shield to a spherical cryogen storage tank under space conditions. The analysis covers these design factors:

1. Combined skin conductance and internal radiation for the shield

2. High emittance bands on the inside and outside of the shield

3. Optimum width of these bands

4. Temperature-varying-absorptance and emittance of the shield's surface

The present analysis extends that of Nichols [5] who imposed constant emittance. And it generalizes the work of Jones and Barry [2, 3] who assumed isothermal radiating zones. We obtained the following results:

1. The high emittance bands and temperature varying emittance combine to lower shield temperatures significantly. Banding allows more heat loss to space. Temperature varying emittance narrows the spread in temperature in going from the sun side to the shadow side of the shield; and it lowers the shield temperature level.

2. Joint inside and outside banding is much more effective than outside banding alone. Optimum inside and outside banding reduces boil-off heat flux by a factor of 4. Outside banding alone gives at most a 12% reduction.

3. Optimum high emittance band width is a weak function of shield-tank separation. The optimum band width is 15° at a separation of one tank diameter, - (tank and shield diameter are the same in this analysis).

THERMAL DESIGN OF INFLATABLE SPHERICAL SHADOW SHIELDS

by D. G. McConnell and J. P. Campbell

Lewis Research Center
National Aeronautics and Space Administration
Cleveland, Ohio

SUMMARY

This report presents the heat transfer from a spherical balloon type shadow shield to a spherical cryogen storage tank.

To find the heat transfer it is necessary to find the temperature profile around the shield. We do this by solving the heat equation for combined radiation and conduction heating of elements of the shield. The equation accounts for the presence of a high emittance band about the shield; and it includes the effect of temperature-varying-emittance. Because of the form of the boundary condition, the equation required an iterative machine solution of the Runge-Kutta type. For small conductance, the temperature is nearly constant on the shadow side of the shield. This constant temperature occurs even though the emittance changes abruptly in crossing the high emittance band. The solution shows that the effect of the high emittance band is to lower the shield's temperature level. Temperature-varying-emittance not only lowers shield temperature; it also narrows the spread in temperature in going from the shield's sun side to its shadow side.

Using the temperature solution and radiation view factors, found separately, we predict the heat flux to the spherical storage tank. In this analysis the shield and tank diameters are equal. We present figures which show the heat flux as a function of width of the high emittance band and shield-tank separation. There is an optimum band width. This optimum band width is a weak function of separation distance, -varying from 15° to 25° as the separation varies from 0 to 4 tank diameters. The heat

transfer calculation further shows that joint inside and outside banding is much more effective than outside banding alone. Two side banding reduces the heat flux by a factor of 4 whereas one side banding gives a reduction of only 12%.

INTRODUCTION

The aim of this paper is to facilitate the design of cryogenic storage systems for spacecraft. Specifically this report gives typical design curves for the heat transfer from a spherical shadow shield to a spherical fuel tank (of equal radius). Curves like these can be useful in the initial design stages in estimating fuel requirements, and in trade-off studies considering various shielding methods.

Interest in long term storage stems from planned interplanetary missions which call for cryogenic fuels such as liquid hydrogen (LH_2) and liquid oxygen (LOX). For example, a Mars mission involves a round trip time of over 400 days. Over such a long period, poor thermal design of the cryogenic storage system could lead to excessive fuel boiloff. On the other hand optimum thermal design gives maximum payload and efficient lift off.

During the planet transfer portion of the flight, the largest external heat source will be the solar heat flux. Smolak, Knoll, and Wallner [1] have shown that shadow shields can greatly reudce solar heating under such conditions. Inflated shadow shields [2, 3] promise low structure weight and, therefore, high shielding efficiency, - in terms of boiloff weight to shield weight.

However, there are other factors which enter into the choice of a thermal control system. Such factors may be the added fuel needed for vehicle orientation required with some systems, the presence of on-board heat

sources, or the presence of several external heat sources. For example, if solar and planetary heat fluxes are present, the designer may consider encapsulation of the cryogen module within a multi-layer foil. In any event, the system for a specific mission must be chosen from several known shielding methods. The results of this report simplify the consideration of spherical balloon shields when making such a choice.

Specifically, this analysis finds the temperature profile around a thin-walled, hollow sphere subject to solar heating. And then, using this profile, the analysis predicts the heat transfer to a spherical storage tank in the shield's shadow. The temperatures result from a solution of the inhomogenous heat equation. The equation accounts for the distribution of the incident heat about the sphere by skin conduction and internal radiation. Furthermore, the equation allows for variable shield surface emittance. The shield emittance may vary with skin temperature, $\epsilon = \epsilon(T)$; and it may vary in a stepwise manner, - viz., banding. Knoll, et al., [4], in their study of flat plate shields have shown that well placed high emittance bands can reduce shield temperature and thereby increase shield efficiency. Herein, we find the effect of high emittance zones (blackened bands) placed on the inside and the outside surface of the shield, on its shadow side. These bands might result from painting a high emittance coating on an otherwise highly reflective material like aluminized mylar. If both the inside and the outside are painted, we call that simple banding. If just the outside is painted, we call that one-side banding.

This paper extends the work of Jones and Barry [2, 3] who also considered spherical, banded shadow shields; and it extends the work of

Nichols [5] who first found the temperature profile around a thin-walled hollow sphere subject to solar heating. Jones and Barry neglected conduction along the skin and, instead, assumed isothermal radiating zones for use in an electrical analogue solution. Nichols included skin conduction but he imposed constant inside and outside surface properties. Thus, his analysis could not include banding and temperature variable emittance.

LIST OF SYMBOLS

A   area

b   thickness of shield's skin

F_{ij} view factor of surface j for flux leaving surface i

H   total radiant flux leaving a surface

I   total radiant flux arriving at a surface

I_{in} internal impinging flux

I_{sol} solar impinging flux $I_{sol} = \Phi \cos \theta$

I_{12} impinging flux due to presence of tank

k   thermal conductivity

L   vector distance between differential radiating areas

Q   heat flux

R   radius of sphere

S   shield-tank separation distance

T   temperature

T_{∞} scaling temperature, temperature to which the shield would come if

$$k = \infty, \ \epsilon_o = \epsilon_i = \epsilon_i' \quad \text{thus} \quad 4\epsilon_{\infty}' \sigma T_{\infty}^4 \equiv \alpha_s^* \Phi$$

$Z(\theta)$ unit step function, $Z(\theta) = 1,\ 0 \leq \theta < \pi/2;\ Z(\theta) = 0,\ \pi/2 \leq \theta \leq \pi$

α absorptance

α_s solar absorptance

$\overline{\alpha}$ average absorptance over inside area of shield $\overline{\alpha} = \dfrac{1}{2} \displaystyle\int_0^\pi \alpha_i \sin \theta'\, d\theta'$

β ratio of inside to outside emittance

ϵ emittance

ϵ_∞ emittance at T_∞

η stretched spatial coordinate

μ dimensionless skin conductance parameter

Φ parallel solar flux vector

φ angle between surface normal and vector L

ψ dimensionless temperature

σ Stefan-Boltzmann constant

θ spatial coordinate - spherical colatitude

Subscripts:

1   refers to shield

2   refers to tank

i   inside

o   outside

TEMPERATURE DISTRIBUTION ANALYSIS

This section gives the main points of the derivation and solution of the heat equation. For more detail, see appendix A.

Figure 1 shows the physical arrangement we analyze. Parallel solar heat flux arrives along the line of centers of the shield and the tank. Figure 1 also shows a control volume containing a typical portion of shield skin. The steady-state energy balance for the control volume is:

$$(\text{Net conduction flux}) = \left\{ \begin{array}{c} \text{leaving radiation} \\ \\ \text{outside + inside} \end{array} \right\} - \left\{ \begin{array}{c} \text{arriving radiation} \\ \\ \text{outside + inside} \end{array} \right\}$$

The arrangement in figure 1 has axial symmetry; further we assume that there is no radial temperature drop through the skin of the shield. Thus, there is conduction only in the θ direction. Hence, the energy balance leads to a heat equation in the form

$$\frac{kb}{R^2 \sin \theta} \frac{d}{d\theta} \left(\sin \theta \frac{dT}{d\theta} \right) = (H_0 + H_i) - (I_{sol} + I_{in} + I_{12}) \tag{1}$$

For definitions, see the List of Symbols. In particular I_{12} is the flux to the shield due to the presence of the tank. In full,

$$I_{12} = \int_{A_2} \left\{ \epsilon_2 \sigma T_2^4 + (1 - \alpha) \int_{A_1} \left[\epsilon_0 \sigma T^4 + (1 - \alpha_0)I_{12} \right] F_{dA_1 dA_2} \right\} dA_1$$

$$\times F_{dA_2 dA_1} \, dA_2 \tag{2}$$

For the problem at hand, I_{12} is negligible because:

1. For a cryogenic tank at Earth orbit, $\sigma T_2^4 \ll I_{sol}$

2. For radiation view factors between spheres

$$\sigma T^4 F_{dA_1 dA_2} F_{dA_2 dA_1} \ll I_{sol} \quad \text{at Earth's orbit.}$$

This is fortunate for in the absence of I_{12} equation (1) becomes an ordinary differential equation for T instead of an integro-differential equation, - viz.

$$\frac{kb}{R^2 \sin \theta} \frac{d}{d\theta}\left(\sin \theta \frac{dT}{d\theta}\right) = (H_o + H_i) - (I_{sol} + I_{in}) \tag{3}$$

After inserting the definitions of the incoming and outgoing fluxes:

$$\left.\begin{aligned} H_o &= \epsilon_o \sigma T^4 + (1 - \alpha_s)I_{sol}, \\ H_i &= \epsilon_i \sigma T^4 + (1 - \alpha_i)I_{int}, \\ I_{sol} &= \Phi \cos \theta \, Z(\theta) \end{aligned}\right\} \tag{4}$$

equation (3) becomes

$$\frac{kb}{R^2 \sin \theta} \frac{d}{d\theta}\left(\sin \theta \frac{dT}{d\theta}\right) = (\epsilon_o + \epsilon_i)\sigma T^4 - \alpha_i I_{in} - \alpha_s \Phi \cos \theta \tag{5}$$

The full derivation (appendix A) shows that for a simply banded sphere, (i.e., $\epsilon_i = \epsilon_o$ or $\beta = 1$)

$$4\overline{\alpha} I_{in} = \alpha_s \Phi \tag{6}$$

Here $\overline{\alpha}$ is the average inside surface absorptance

$$\overline{\alpha} \equiv \frac{1}{2} \int_0^t \alpha_i \sin \theta \, d\theta \tag{7}$$

Notice that α_i depends upon position not only because of banding but also because it depends on temperature which is a function of position. The final form of the heat equation is

$$\frac{kb}{R^2 \sin \theta} \frac{d}{d\theta}\left(\sin \theta \frac{dT}{d\theta}\right) = (\epsilon_o + \epsilon_i)\sigma T^4 - \left(\frac{\alpha_i}{\overline{\alpha}}\right)\left(\frac{\alpha_s \Phi}{4}\right) - \alpha_s \Phi \cos \theta \, Z(\theta) \tag{8}$$

We follow Nichols and use as a scaling temperature, $T_\infty = \left[(\alpha_s \Phi)/(4\epsilon_\infty \sigma)\right]^{1/4}$. This is the temperature to which the shield would come if it had infinite conductance, and no high emittance band. For thermal variation of emittance and absorptance of unblackened areas of the shield, we assume:

$$\epsilon_i = \left(\frac{\epsilon_\infty}{T_\infty}\right) T \quad \text{and} \quad \epsilon_i = \epsilon_o, \quad \epsilon = \alpha$$

The only outside absorptance in the problem is α_s, the solar absorptance. For banded (blackened) zones of the shield we assume

$$\alpha_i = \alpha_o = \epsilon_i = \epsilon_o = 1$$

Upon substitution of the terms:

$$\Psi \equiv \frac{T}{T_\infty}; \quad \mu = \frac{kb}{\epsilon_\infty \sigma T_\infty^3 R^2}$$

the heat equation becomes

$$\frac{\mu}{\sin\theta} \frac{d}{d\theta}\left(\sin\theta \frac{d\Psi}{d\theta}\right) = 2\Psi^5 - \left(\frac{\epsilon_\infty}{2}\right)\Psi - 4\cos\theta \; Z(\theta) \tag{10a}$$

The boundary conditions are:

$$\frac{d\Psi}{d\theta} = 0 \quad \theta = 0; \quad \frac{d\Psi}{d\theta} = 0, \quad \theta = \pi \tag{10b}$$

Equations 10(a), and (b) require an iterative solution since the constant $\overline{\alpha}$ can only be found from the solution. Because of the form of the boundary conditions (10b) we found a numerical solution using a two-point

Runge-Kutta technique. The solutions of equations 10(a), and (b), are shown in figure 2. With the temperature profile known it is possible to calculate the heat transfer to the tank.

Heat Transfer

In finding the heat transfer, we assume the tank to be isothermal (i.e., T_2 independent of θ_2) and also that $T_2 \ll T_1$. In this case, the net heat transfer from the shield (body one) to the tank (body two) is

$$Q_{12} = \int_{shield} \frac{\alpha_2 F_{12} \epsilon_1 \sigma T_1^4 \, dA_1}{1 - (1 - \alpha_1)(1 - \alpha_2) F_{12} F_{21}} \tag{12}$$

where the radiation view factor is given by:

$$F_{12} \, dA_1 \equiv \int_{A_1} \frac{\cos \varphi_1 \cos \varphi_2 \, dA_2 \, dA_1}{\pi L^2}$$

Equation (12) gives the heat transfer as a function of shield emittance and shield tank separation. The emittance variation $\epsilon_1 = \epsilon_1(\theta)$ accounts for the high and low emitting portions of the shield, - due to banding and temperature variation. The shield-tank separation appears in the view factor. We present the view factors separately in [6].

DISCUSSION OF RESULTS

Figure 2 shows the effect of skin conductance, μ, on the dimensionless temperature distribution around the shield. Figure 2(a) is for constant unblackened surface emittance. In finding these temperatures we used a representative value for emittance, such as that of aluminized mylar $\epsilon = 0.045$ over the unblackened portion. We used an emittance of 1 for the 15°

blackened band. Figure 2(b) shows the temperature profile for the case where emittance varies with temperature. Here we used $\epsilon_\infty = 0.0585$. The relationship between the cases of constant and variable emittance is shown in appendix B.

Figures 2(a) and (b) both show that the temperature profile for $\mu = 0.1$ is only slightly different from the profile for $\mu = 0$. For materials and skin thicknesses of technical interest, μ is between 10^{-3} and 10^{-5}. Therefore for the rest of this paper, we discuss only the temperatures and heat transfer for zero shield conductance. This has the advantage that for $\mu = 0$, the heat equation becomes algebraic and its solution is much easier.

Finally, note that both figures 2(a) and (b) show a uniform temperature on the shadow (tank) side of the shield, for $\mu = 0$. Uniform temperature occurs even though the emittance changes abruptly at $\theta = \pi/2$ and $\theta = \frac{\pi}{2} + \theta_b$. This supports the Jones and Barry assumption [2, 3] of isothermal radiating zones. However, the present solution has the advantage of giving the band temperatures explicitly.

Figures 3 and 4 compare the temperature profile for five analytical cases. As shows in the legends of the figures, these five cases are combinations of one side or two side banding with and without temperature variable unbanded emittance. The cases as defined in figure 3 and 4 will be used throughout this discussion. Case I, the standard, is the Nichols profile [5] for constant absorptance and emittance (i.e., neither banding nor $\epsilon = \epsilon(T)$).

In figure 3, profile II shows that banding and temperature variable emittance lower shield dimensionless temperature, ψ, relative to case I. The decrease in dimensionless temperature, ψ, results directly from banding. In addition, the scaling temperature, T_∞, for case II is lower than for case I. This results from the increase in emittance with increasing temperature. Thus the dimensional temperature $T = T_\infty \psi$ will be lower in case II than in case I.

Further, profiles II and III, in figure 3, are continuous even though the emittance is discontinuous crossing the blackened band. For $\mu = 0$, the temperatures could be discontinuous. Here they are not, for the following reasons. Outside blackening increases the ability to lose heat to space; but this greater heat loss is just balanced by greater heat gain from internal blackening. Thus the temperatures are continuous. Profile IV, for outside black band only, strengthens this argument; because it shows a sharp drop in temperature at the blackened band.

Figure 4 shows how temperature varying emittance alters profile I without targetting. Notice that the spread in temperature from the sun side to the tank side is smaller when $\epsilon = \epsilon(T)$.

Figure 5 shows how the heat transfer from shield to tank varies with high emittance band width θ_b. For clarity, we present these curves in dimensionless form. Shield temperature goes down as θ_b grows, but the emissive power of the shield increases with θ_b. These two opposing effects give rise to an optimum band width (minimum Q_{12} for a particular S value). However, the view factor, and thereby the effective emittance,

depends upon shield tank separation. So the optimum band width also depends upon separation distance. The optimum band width varies from 12° for a separation of 8R to 21° for zero separation. At the optimum band width, targetting can reduce the heat transfer by as much as 75% (at zero separation). This reduction decreases with increasing separation. The reduction in heat transfer is 60% at a separation S = 8R.

Figure 5 further shows that, increases in bandwidth beyond optimum lead to heat transfer Q_{12} almost twice the unbanded value when $\theta_b = \pi/2$.

Figure 5 shows how the boil-off heat flux varies with high emittance band width and shield tank separation distance. These curves are representative of design curves which might be used in choosing between shielding methods. Since the curves require particular emittance values $(\epsilon_\infty, \epsilon_0)$ they are not general.

The ordinate of figure 5 is related to the solar heat flux as follows

$$\frac{Q_{12}}{\sigma T^4} = \frac{Q_{12}}{\frac{1}{4}\left(\frac{\alpha_s}{\epsilon_\infty}\right)\Phi} = \frac{4Q_{12}}{\left(\frac{\alpha_s}{\epsilon_\infty}\right)\Phi}$$

It is clear from figure 5 that one side targetting is far less effective than two side targetting in reducing heat flux.

CONCLUSIONS

1. Use of a high-emittance band on spherical shadow shields decreases heat flux to a spherical shielded body by as much as a factor of 4. For cases considered here, the optimum high emittance band width is between 12° and 25° for separation of zero to eight tank radii.

2. Banding and temperature variable emittance both decrease shield temperature level, and hence reduce the heat flux. Further, variable emittance narrows the spread in temperature about the shield.

3. Having high emittance bands inside and outside is much more effective in reducing shield temperature than outside banding alone.

4. For small conductance ($\mu < 10^{-1}$), shield temperature is nearly constant on the shadow side. This supports the assumption used in the design method of Jones and Barry [2, 3]. However, the present calculations are more simple and direct than those of references 2 and 3.

APPENDIX A

DERIVATION OF HEAT EQUATION

This section presents the full derivation of the heat equation, equation (10) of the main text.

From the energy balance

$$\frac{kb}{R^2 \sin\theta} \frac{d}{d\theta}\left(\sin\theta \frac{dT}{d\theta}\right) = (H_o + H_i) - (I_{sol} + I_{in} + I_{12}) \tag{A1}$$

The symbol H stands for the total amount of flux leaving a surface, (i.e., emitted plus reflected). For example

$$H_i = \epsilon_i \sigma T^4 + (1 - \alpha_i)I_{in}; \quad H_o = \epsilon_o \sigma T^4 + (1 - \alpha_s)I_{sol} + (1 - \alpha)I_{12}$$

The symbol I_{12} is the total flux impinge on the shield (body 1) because of presence of the tank (body 2)

$$I_{12} = \int \left\{\epsilon_2 \sigma T_2^4 + (1 - \alpha_2)\int\left[\epsilon_o \sigma T^4 \right.\right.$$
$$\left.\left. + (1 - \alpha_1)I_{12}\right]F_{dA_1 dA_2} dA_1\right\} F_{dA_2 dA_1} dA_2 \tag{A2}$$

The inside impinging flux is

$$I_{in}(\theta) = \int \left[\epsilon_i \sigma T^4(\theta) + (1 - \alpha_i)I_{in}(\theta') \right] F_{dA'dA} \, dA_i' \qquad (A3)$$

From Nichols [5]

$$dA_i' = 2\pi R^2 \sin \theta' d\theta'; \quad F_{dA'dA} = \frac{1}{4\pi R^2}$$

and

$$I_{in}(\theta) = \frac{1}{2} \int_0^\pi \left[\epsilon_i \sigma T^4(\theta') + (1 - \alpha_i)I_{in}(\theta') \right] \sin \theta' \, d\theta' \qquad (A4)$$

Thus I_{in} is independent of θ.

$$I_{in} = \frac{1}{2} \int_0^\pi \left[\epsilon_i \sigma T^4(\theta') \right] \sin \theta' \, d\theta' + (1 - \overline{\alpha})I_{in} \qquad (A5)$$

$$\overline{\alpha} \equiv \frac{1}{2} \int \alpha_i \sin \theta' \, d\theta'$$

Return to equation (A1) and consider I_{12}. For a cryogenic storage tank $\sigma T_2^4 \ll I_{sol}$. Also for two spheres $(\epsilon_o \sigma T^4 F_{dA_2 dA_1} F_{dA_1 dA_2} \ll I_{sol}$. So neglect I_{12} in equation (A1). Then (A1) becomes

$$\frac{kb}{R^2 \sin \theta} \frac{d}{d\theta} \left(\sin \theta \frac{dT}{d\theta} \right) = (\epsilon_o + \epsilon_i)\sigma T^4 - \alpha_i I_{in} - \alpha_s I_{sol} \qquad (A6)$$

Use (A6) to replace $\epsilon_i \sigma T^4$ under the integral in (A5)

$$\overline{\alpha}I_{in} = \frac{1}{2}\int_0^{\pi}\left(\frac{\epsilon_i}{\epsilon_i + \epsilon_o}\right)\left[\frac{kb}{R^2 \sin \theta'}\frac{d}{d\theta'}\ \sin \theta'\frac{dT}{d\theta'} + \alpha_i I_{in}\right.$$

$$\left. + Z(\theta)\alpha_s \Phi \cos \theta'\right]\sin \theta'\ d\theta' \qquad (A7)$$

Once we specify the variation of ϵ_i and ϵ_o over the shield, the integral can be performed to make (A6) an ordinary equation. Suppose that ϵ is a linear function of temperature; and let $\epsilon_i = \beta\epsilon_o$. Then

$$\frac{\epsilon_i}{\epsilon_i + \epsilon_o} = \frac{\beta}{1 + \beta}$$

Then

$$I_{in} = \frac{\beta\alpha_s\Phi}{4\overline{\alpha}} \qquad\qquad (A8)$$

For

$$\beta = 1, \qquad 4\alpha I_{in} = \alpha_s\Phi$$

As a result (A6) becomes

$$\frac{kb}{R^2 \sin \theta}\frac{d}{d\theta}\left(\sin \theta\frac{dT}{d\theta}\right) = (1 + \beta)\epsilon_o \sigma T^4 - \left(\frac{\alpha_i}{\overline{\alpha}}\right)\beta\alpha_s\Phi - \alpha_s\Phi \cos \theta \qquad (A9)$$

Using

$$4\epsilon_{\infty}\sigma T_{\infty}^4 = \alpha_s\Phi; \quad \mu = \frac{kb}{R^2 \epsilon_{\infty}\sigma T_{\infty}^3}$$

$$\frac{\mu}{\sin \theta}\frac{d}{d\theta}\left(\sin \theta\frac{d\psi}{d\theta}\right) = (1 + \beta)\left(\frac{\epsilon_o}{\epsilon_{\infty}}\right)\psi^4 - \left(\frac{\alpha_i}{\overline{\alpha}}\right)\beta - 4\cos \theta \qquad (A10a)$$

for

$$0 \le \theta \le \frac{\pi}{2}$$

and

$$\frac{\mu}{\sin \theta} \frac{d}{d\theta} \left(\sin \theta \frac{d\psi}{d\theta} \right) = (1 + \beta)\left(\frac{\epsilon_o}{\epsilon_\infty}\right)\psi^4 - \left(\frac{\alpha_i}{\overline{\alpha}}\right)\beta \tag{A10b}$$

for

$$\frac{\pi}{2} \le \theta \le \pi$$

In the main text we assume $\beta = 1$ and $\alpha_i = \epsilon_i$. The assumption $\beta = 1$ implies that the outside surface is prepared exactly like the inside surface. For example, doubly aluminized mylar painted black inside and outside on the shadow side (viz. $\pi/2 \le \theta \le \pi/2 + \theta_b$). If in addition to $\beta = 1$, we assume $\epsilon = (\epsilon_\infty/T_\infty)T = \epsilon_\infty\psi$, it follows that

$$\frac{\mu}{\sin \theta} \frac{d}{d\theta} \left(\sin \theta \frac{d\psi}{d\theta} \right) = 2\psi^5 - \left(\frac{\epsilon_\infty}{\overline{\alpha}}\right)\psi - 4\Big[Z(\theta)\Big]\cos \theta \tag{A11}$$

For the case of outside targetting alone, equation (A8) does not have such a simple form for the ratio $(\epsilon_i/(\epsilon_i + \epsilon_o))$ does not remain constant. Suppose, for instance, that $\epsilon_i = \epsilon_o = $ constant except over the targetted band where $\epsilon_o = 1$. Then

$$\alpha_i I\left[\frac{2(1 + \epsilon_i) + \sin \theta_b(1 - \epsilon_i)}{4(1 + \epsilon_i)}\right] = \frac{kb}{4R^2}\left[\left(\frac{dT}{d\theta}\right)\Bigg|_{\pi/2-} - \frac{2\epsilon_i}{(1 + \epsilon_i)}\left(\frac{dT}{d\theta}\right)_{\pi/2+}\right]$$

$$- \frac{kb}{4R^2}\cos \theta_b\left\{\left(\frac{dT}{d\theta}\right)_{[(\pi/2)+\theta_b]+} - \frac{2\epsilon_i}{1 + \epsilon_i}\left(\frac{dT}{d\theta}\right)_{[(\pi/2)+\theta_b]-}\right\} + \frac{\alpha_s\Phi}{8} \tag{A12}$$

The symbol $(dT/d\theta)_{\pi/2-}$ stands for the derivative approaching $\pi/2$ from the left; and $(dT/d\theta)_{\pi/2+}$ implies the value approaching from the right. However for $k \neq 0$ but continuous, equation (A6) implies that [8]

$$\left(\frac{dT}{d\theta}\right) = \frac{R^2}{kb}\frac{1}{\sin\theta}\int_0^\theta \left[(\epsilon_0 + \epsilon_i)\sigma T^4 - \alpha_i I_{in} - \alpha_s I_{sol}\right]\sin\theta' \, d\theta'$$

Even if the integrand has jumps, the right hand side must be continuous; consequently the left hand side must be continuous. Then (A12) can be placed in (A6) to obtain

$$\frac{\mu}{\sin\theta}\frac{d}{d\theta}\left(\sin\theta\frac{d\psi}{d\theta}\right) = \frac{(\epsilon_0 + \epsilon_i)}{\epsilon_\infty}\psi^4 - \frac{(1 + \epsilon_i)}{2(1 + \epsilon_i) + (1 - \epsilon_i)\sin\theta_b}$$

$$\times \left\{2 + \mu\left(\frac{1 - \epsilon_i}{1 + \epsilon_i}\right)\left[\left(\frac{dT}{d\theta}\right)_{\pi/2-}\cos\theta_b\left(\frac{dT}{d\theta}\right)_{[(\pi/2)+\theta_b]}\right]\right\} - 4\,Z(\theta)\cos\theta \quad (A13)$$

This is the heat equation where only the outside is blackened. It requires an iterative solution.

APPENDIX B

EVALUATION OF T_∞ FOR ϵ A LINEAR FUNCTIONS OF TEMPERATURE

We assume as an example, a variation of emittance with temperature of the form $\epsilon = (\epsilon_\infty/T_\infty)T$ for all temperature ranges of interest. This form was motivated by the form given by Siegel and Howell [6] for temperatures around room temperature] $\epsilon = (\epsilon_{273}/273)T$. We used this latter equation to find ϵ_∞ for case II as follows:

$$\alpha_s \Phi = 4\epsilon_\infty \sigma T_\infty^4$$

$$\epsilon_\infty = \left(\frac{\epsilon_{273}}{273}\right) T_\infty$$

$$T_\infty^5 = \frac{\alpha_s \Phi}{4\sigma \left(\frac{\epsilon_{273}}{273}\right)}$$

For ϵ_{273} we used the handbook value for aluminum foil, $\epsilon = 0.045$. This led to

$$\epsilon_\infty = 0.0585$$

$$T_\infty = 355^O \text{ K}$$

For case III we used $\epsilon = 0.045$ and $T_\infty = 379^O$ K.

APPENDIX C

MAGNITUDE OF HEAT FLUX TO THE SHIELD DUE TO THE TANK

The analysis of the temperature profile neglected the heat flux to the shield due to the presence of the tank. The terms in equation (10) are all of magnitude $\epsilon \sigma T_1^4$. Since the tank is at cryogenic temperatures (say 20° K),

$$\left(\frac{T_2}{T_1}\right)^4 \ll 1$$

and direct emission from tank to shield is negligible. The tank reflects heat from the shield back to the shield. This heat is

$$Q = \frac{\left(\epsilon \sigma T_1^4\right) F_{12} F_{21} (1 - \alpha_2) \alpha_1}{1 - F_{12} F_{21} (1 - \alpha_2)(1 - \alpha_1)}$$

Thus the relative size of this term is

$$\frac{F_{12}F_{21}(1 - \alpha_2)\alpha_1}{1 - F_{12}F_{21}(1 - \alpha_2)(1 - \alpha_1)}$$

There are four cases to consider. These are the combination of the tank reflecting heat from the shiny or blackened portions of the shield back to the shiny or blackened portions of the shield. In each of the four combinations, the relative size of the flux was less than 10^{-3} for a shield-tank separation of one tank diameter. Thus there was small error in neglecting the presence of the tank in calculating the shield temperature profile.

REFERENCES

1. G. R. Smolak, R. H. Knoll, L. E. and Wallner, "Analysis of Thermal-Protection Systems for Space-Vehicle Cryogenic-Propellant Tanks," NASA TR R-130, 1962.

2. L. R. Jones, et. al., "A Study of Lightweight Shadow Shields for Cryogenic Space Vehicles," General Dynamics/Fort Worth Reptort FZA-395 (NASA CR-60741), January 31, 1965.

3. L. R. Jones and D. G. Barry, "Lightweight Inflatable Shadow Shields for Cryogenic Space Vehicles," Journal of Spacecraft and Rockets, vol. 3, no. 5, May, 1966, pp. 722-728.

4. R. H. Knoll, E. R. Bartoo, and R. J. Boyle, "Shadow Shield Experimental Studies." Paper presented of Conference on Long-Term Cryo-Propellant Storage in Space, NASA George C. Marshall Space Flight Center, Huntsville, Alabama, Oct. 12-13, 1966.

5. L. D. Nichols, "Surface-Temperature Distribution on Thin-Walled Bodies Subjected to Solar Radiation in Interplanetary Space," NASA TN D-584, October, 1961.

6. J. P. Campbell and D. G. McConnell, "Radiant Interchange Configuration Factors for Spherical and Conical Surfaces to Spheres," Proposed NASA Technical Note.

7. R. Siegel and J. R. Howell, "Thermal Radiation Heat Transfer. Vol. I - The Blackbody, Electromagnetic Theory, and Material Properties," Proposed NASA Special Publication.

8. T. M. Apostol, Mathematical Analysis, Addison-Wesley Publishing Co., Reading, Mass., 1957, p. 214.

$$\varepsilon_0 \sigma T*4$$

Solar heat flux

Conduction heat out

Conduction heat in $I(\theta)$ $H(\theta)$

θ_b

Solar
radi-
ant
heat
flux

Hollow spherical
shadow-shield
surface 1

Spherical
cryo-tank
surface 2
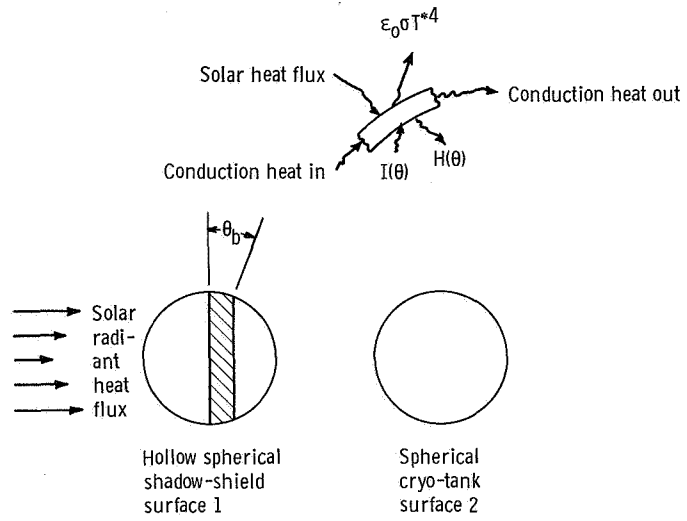
Figure 1. - Spherical shield analysis geometry.
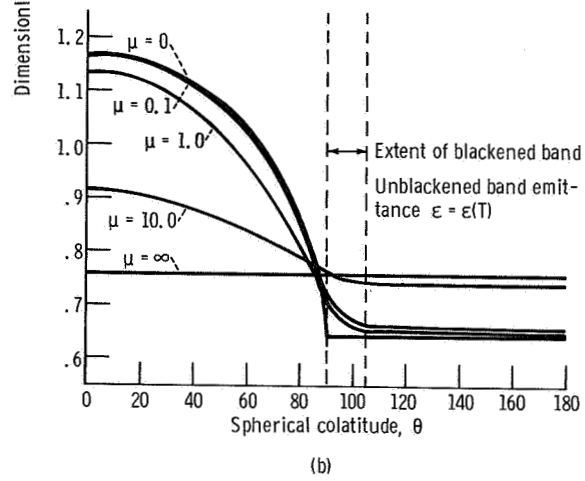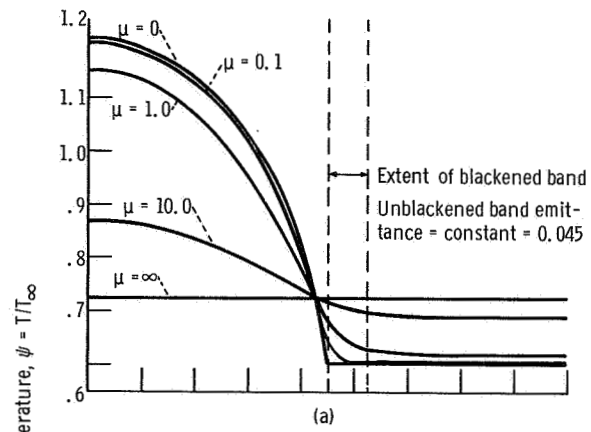
Figure 2. – Effect of skin conductance on temperature profile.

Case
I   No blackening (Nichols [5]) ε = const.
II Black band, inside and out
    plus tempeaature variable
    emittance, $\varepsilon = \varepsilon_\infty \psi$
III Black band, inside and out
    ε independent of ψ
IV Black band outside only,
    ε independent of ψ
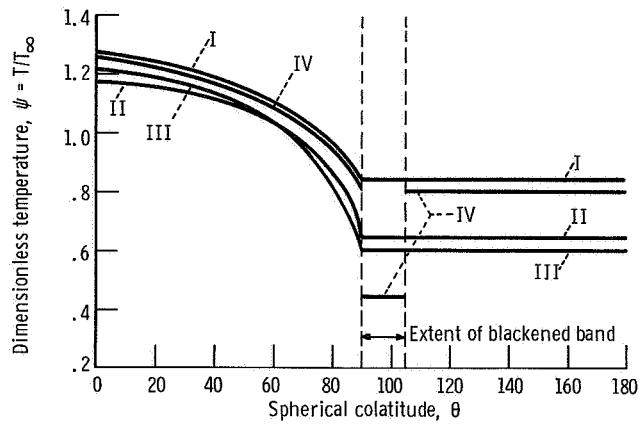
Figure 3. - Effect of targetting on dimensionless temperature profile (μ = 0, θ_b = 15°).

I Constant emittance (Nichols [5])
V Emittance given by $\varepsilon = \varepsilon_\infty \psi$

No blackening in either case
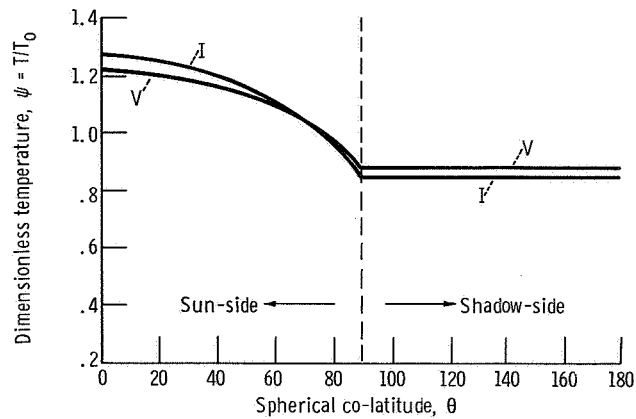
Figure 4. - Effect of temperature varying emittance ($\varepsilon(t)$) on dimensionless temperature profile (μ = 0).
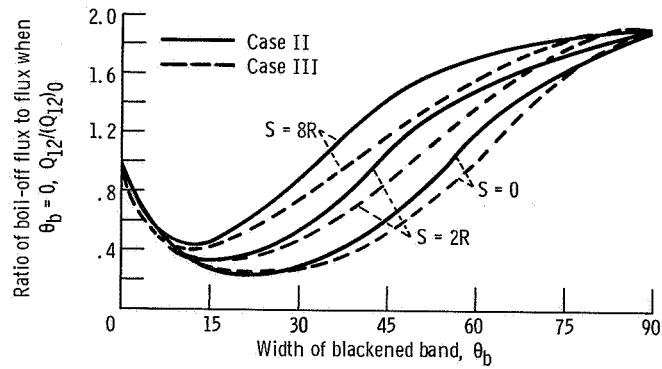
Figure 5. - Relative effect of targetting on boil off heat flux.
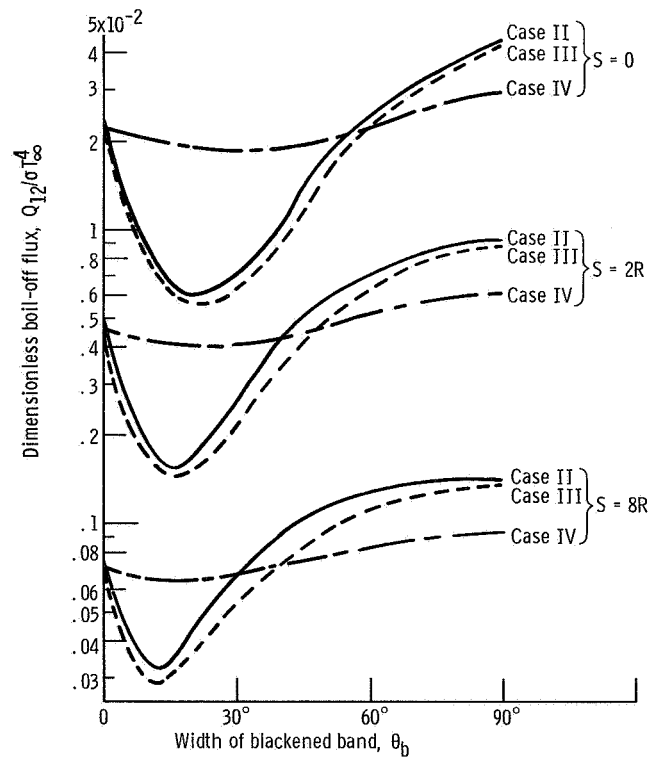
Figure 6. - Boil off flux as effected by targetting and shield-tank separation.